Applied Physics Express 5 (2012) 051701
DOI: 10.1143/APEX.5.051701

Tailoring Monodomain in Blue Phase Liquid Crystal by Surface Pinning Effect

Prasenjit Nayek, Heon Jeong, Hye Ryung Park, Shin-Woong Kang, Seung Hee Lee*, Heung Shik Park[1], Hyuck Jin Lee[1], and Hee Seop Kim[1]

Department of BIN Fusion Technology and Department of Polymer-Nano Science and Technology, Chonbuk National University, Jeonju, Jeonbuk 561-756, Republic of Korea
[1]*LCD Research Center, LCD Division of Samsung Electronics, Giheung, Gyeonggi 446-711, Republic of Korea*

Received February 21, 2012; accepted April 19, 2012; published online May 10, 2012

Surface pinning effect of the optically isotropic, blue phase liquid crystal (BPLC) has been studied. Polycrystalline, platelet, multi-domain topological defects without surface treatment have been transformed to uniform monodomain in rubbed surfaces of the cell. The operating voltage was reduced by 27%, owing to a dramatic increase in the Kerr constant. Hysteresis was reduced by 63%, whereas the transmission efficiency gets doubled. The surface anchoring effect on the blue phase plays a significant role in the elastic free energy, coherence length and topological defects. BPLC displays with a low operating voltage, and reduced hysteresis can be realized with surface treatment.

Blue phases (BPs) are thermodynamically stable, three-dimensionally self assembled, soft photonic, and technically sound liquid crystalline phases which depict a very short temperature range, and typically arise just below the clearing temperature and above the chiral nematic phase (N*). Among the three types of stable BPs, two of them, BP I and BP II, exhibit cubic symmetry in which the orientational order is periodic and long range in three dimensions.[1)] BP I has a body-centered cubic structure, whereas BP II has a simple cubic structure. The BP I director field possesses the symmetry group O^8 ($I4_132$) and BP II, O^2 ($P4_232$).[2)] The symmetry of BP III phase is the same as that of the isotropic phase.[3–7)] The sub-millisecond response time could be helpful to construct a more realistic moving image quality with high image-driving speed without any overdrive circuit.[8)] Fast grey–grey response time[9)] minimizes the motion-image blur and enables field-sequential-color displays without color filters if an RGB LED backlight is used. The transmittance of BPLC is insensitive to the cell gap as long as it exceeds 2–3 μm.[10)] This cell gap insensitivity is mainly advantageous for large-panel liquid crystal displays (LCDs) from the perspective of manufacturing yield.[11,12)]

Recently, Kikuchi *et al.*[13)] have reported the polymer-stabilized BP (PSBP) to achieve the wide temperature range but there are also some disadvantages. High driving voltage[14,15)] and low contrast ratio (due to residual birefringence) are the impediments that have to be overcome. Hysteresis is also one of the major disadvantages in commercializing it. Hysteresis is not affected by polymer concentration but depends on the host liquid crystal and chiral dopants.[16)] Thus, it is important to study the hysteresis in the pure BP sample. In our recent work,[17)] we have observed a hysteresis-reduced optically isotropic state with completely distinct switching routes, determined by the frequency of the electric field applied. However, the characteristics is associated with ionic mobility.

In this paper, we have focused on the effect of surface treatment on the electro-optic characteristics of BPLC. The hysteresis, threshold voltage, operating voltage, Kerr constant, and transmission between homogeneously aligned, rubbed polyimide (PI) surfaces and alignment layer less, untreated cell have compared. A topological defect-free, uniform, monodomain has been achieved, which is strongly desirable for displays as well as photonic[18,19)] applications.

For experimental purposes, commercially available BPLC LCMS-BP-081009-1 (LC Matter), which consists of the host nematic liquid crystal mixture of cyanobiphenyl and cyanoterphenyl group, was used. The host NLCs have dielectric anisotropy, $\Delta\varepsilon = +14$–17, birefringence, $\Delta n = 0.25$–0.28, and mixed with two chiral dopants, ZLI4572 (8 wt %) and CB15 (22 wt %). We have used in-plane switching (IPS) electrodes [width (w)/gap (l) is 4 μm/4 μm and cell gap is 5 μm] for the electro-optic measurements. Surface treatments were performed by coating the inner surfaces of the glass substrates with commercially available planar polyimide for the IPS mode with thickness of 1000 Å. These PI layers are mechanically buffed to produce uniform pre-tilt angle. Top and bottom electrodes are rubbed anti-parallely. The textures of BPLC were taken by using polarizing optical microscopy (POM) system, Nikon DXM1200. The cooling rate of the LC cells was controlled using a temperature controller (Linkam TMS 94) at 0.1 °C/min. The cell has been driven with a variable amplitude, square wave pulse with a frequency, of 1 kHz from a function generator (Tektronix AFG3022) connected to an amplifier. The optical transmittance was measured using an image analyser *i*-solution (*i*M Technology).

Figure 1(a) shows the phase sequence of the BP sample in a non surface treated cell. The isotropic-to-BP I transition takes place at 66.6 °C and the BP I-to-chiral nematic transition is observed at 63 °C. Thus, the BP I temperature range, ΔT_{BPI} is 3.6 °C. The domain size and platelets are not well distributed in the cell. The untreated glass plates do not provide azimuthal direction of LC anchoring on surfaces so that droplets are formed and coalesce during the isotropic-to-BP I transition. Figure 1(b) shows the phase sequence of the surface-treated, i.e., rubbed PI cells with the same electrode geometry. The isotropic-to-BP I transition takes place at 65.5 °C and BP I-to-chiral nematic transition is observed at 62 °C. Thus, the BP I temperature range, ΔT_{BPI} is 3.5 °C, which is almost the same. Surprisingly, uniform monodomain is achieved in the homogeneously aligned cell. Now, certainly questions such as how it arises and what are the causes of that need to be answered. For the explanation of this phenomenon we referred to the recent theoretical results published by Tiribocchi *et al.*[20)] Homogeneous anchoring at the surfaces of the cell, deformed the networks of

*E-mail address: lsh1@chonbuk.ac.kr

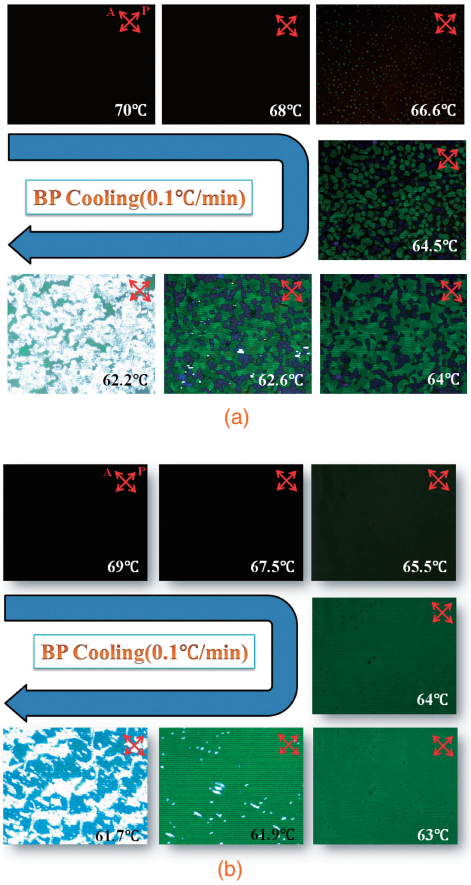

Fig. 1. Polarizing optical microscopic textures during the cooling of the sample from the isotropic state at the rate of 0.1 °C/min (a) in the untreated IPS cell, (b) in the homogeneously aligned, IPS cell.

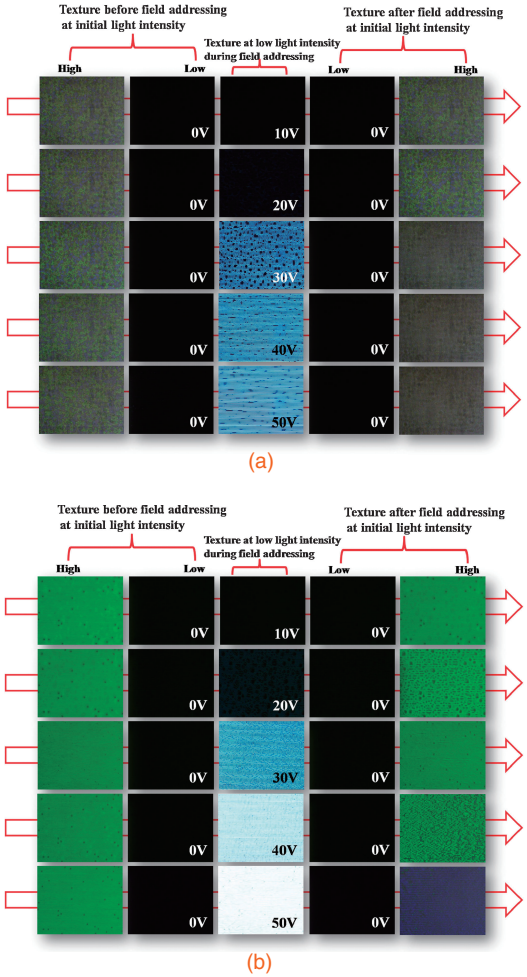

Fig. 2. Polarizing optical microscopic textures showing transmission before and after the electric field addressing at different voltages: (a) non-surface treated IPS cell and (b) homogeneously aligned, IPS cell. Homogeneously aligned, cell can better withstand the voltage than the non-surface treated IPS cell and shows less light leakage due to less electrostriction for the same applied voltage.

disclinations and reconstruct in such a way that they join just above the surface to avoid the surface and then the surface is topologically defect-free.

In the BPLC in which an optically isotropic media exists under a crossed polarizer, the transmittance of the device associated with the induced phase retardation is described using

$$T(\lambda) = T_0(\lambda)\sin^2 2\psi(V)\sin^2\left[\frac{\pi d_i \Delta n_i(V)}{\lambda}\right], \qquad (1)$$

where ψ is the voltage-dependent angle between the transmission axes of the crossed polarizer and the induced optic axis of the BPLC, d_i is the thickness of BPLC layer associated with Δn_i, and λ is the wavelength of an incident light. In order to have maximum transmission, ψ and $d_i\Delta n_i$ should be equal to 45° and $\lambda/2$, respectively. In other words, the field direction that induces the birefringence should always be 45° with respect to the polarizer.

Figure 2(a) shows the textures of the untreated cell for different applied voltages. First column [Fig. 2(a)] depicts the texture of the non surface treated cell when light intensity of POM is high. The second column is the texture under low light intensity, and under this condition, the textures are invisible and look black. The transmitted light through the cell for different voltages is shown in the third column of Fig. 2(a). The fourth column is the texture after the field addressing and in the high light intensity. It is noticeable that, for 10 and 20 V_{rms}, the textures are the same as those before the field addressing, whereas the blackish textures after field addressing of 30, 40, and 50 V_{rms} are not the same. This indicates that the platelet structure has been destroyed due to the high electric field. Similarly, in Fig. 2(b), the middle column shows the textures for different voltages applied to the cell. The Light intensity increases with increasing applied voltage due to the electric field induced birefringence change. It is also noticeable that the textures before and after electric field addressing remain unaffected up to 40 V_{rms}. Therefore, we can infer that for the homogeneously aligned rubbed cell, the voltage induced deformation of the BP structure is less than that of the alignment less cell. At 50 V_{rms}, the texture shows a blue color after electric field is withdrawn. This indicates the initial BP structure fails to restore under high voltage addressing. Nevertheless, compared to the non-rubbed cell where BP is destroyed completely, the texture is less deformed and uniform.

Figure 3 shows voltage-dependent transmittance curves (V–T) with ascending and descending voltages. For the untreated cell [see Fig. 3(a)], we have found that there is no saturation of transmitted light intensity for the application of 50 V_{rms}, which indicates that the applied voltage is not

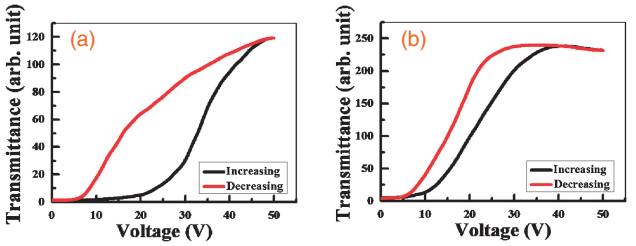

Fig. 3. Voltage dependent transmission curve: (a) non-surface treated IPS cell and (b) rubbed PI, IPS cell. The surface treated, rubbed cell has higher transmission than the untreated cell for the same cell thickness and applied voltage.

Table I. Compared hysteresis for rubbed PI and untreated IPS cells under different applied voltages (units: V).

	Hysteresis (ΔV_{50})			
	20	30	40	50
Untreated cell	1.52	6.77	7.85	15.3
Rubbed PI cell	0.95	3.29	5.06	5.7

sufficient to reach up to the maximum transmission level. We can further infer that the operating voltage in the untreated cell is larger than 50 V_{rms}. We have found that the threshold voltage V_{th} [T_{10}] is 24.4 V_{rms} and the operating voltage V_{90} [T_{90}] is 43.6 V_{rms}. We have defined the hysteresis from the voltage difference at 50% of the maximum transmission level (ΔV_{50}). We found that ΔV_{50} is 15.3 V_{rms}, which is not favorable for display applications. On the other hand, Fig. 3(b) depicts the V–T graph for the homogeneously aligned cell. The V–T graph shows saturation of transmission at voltages lower than those of the previous untreated cell. That means that a lower operating voltage is achieved in the rubbed cell. We have measured the threshold voltage V_{th} [T_{10}] is 12.3 V_{rms} and operating voltage V_{90} [T_{90}] is 32 V_{rms}. Hysteresis is reduced dramatically to about 5.7 V_{rms}. It is worthy to say that V_{th} for the rubbed cell is reduced by 50%, V_{90} is reduced by 27%, and hysteresis is reduced by 63%, which is remarkable. The reason for the less hysteresis in the rubbed cell may be due to anchoring force, which exerts an additional restoration force[12] and helps BPLC molecules to come back to the initial position. Table I also shows the voltage-dependent hysteresis for both cases. It clear from the table that hysteresis is less for the homogeneously aligned cell rather than non treated cell upto 50 V_{rms}. We have measured the Kerr effect,[21] which is a non-linear, quadratic electro-optic effect that could be induced by the application of an electric field. The magnitude of the birefringence induced via the Kerr effect could be expressed as

$$\Delta n_{\text{induced}} = \lambda K E^2, \tag{2}$$

where $\Delta n_{\text{induced}}$ is the induced birefringence λ is the wavelength of light, and K is the Kerr constant. Figure 4(a) shows the difference in the transmission level. The rubbed, homogeneously aligned cell has far better transmission than the untreated cell. Figure 4(b) depicts the Δn versus E^2 graph. From this graph, we have calculated the Kerr constant for both cases. The calculated Kerr constant is 0.54 nm/V^2 for the untreated cell whereas for the rubbed cell, this value

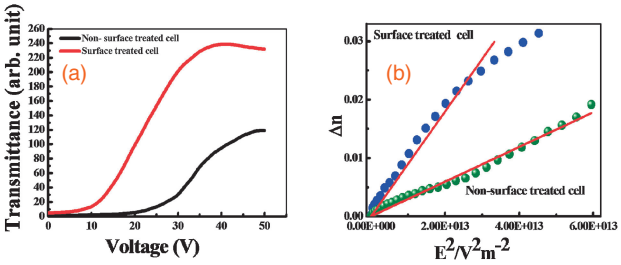

Fig. 4. (a) Compared V–T curve for rubbed PI and untreated cells, (b) electric-field-induced birefringence (Δn) against the square of the electric field for non-treated cell (green circle) and rubbed PI cell (blue circle). The rubbed PI cell has a higher slope so its Kerr constant is also higher.

increases dramatically to 1.63 nm/V^2. The increase is 67% with respect to the untreated cell. As we know, the Kerr constant is proportional to the product $\Delta\varepsilon \times \Delta n$, i.e., the product of dielectric anisotropy and birefringence of the material. However, in our case, it is very anomalous that although we have used the same sample, only the rubbed PI surface increases the Kerr constant by 67%. We know that the Kerr effect of a nematogen is proportional to the square of the coherence length, ξ^2.[22] In our case, ξ becomes a coherence length in which BP I lies in the same plane instead of the length for one cubic structure, so that it becomes relatively larger than that of the untreated cell and shows a higher Kerr constant.

In conclusion, we have found that surface treatment of the BPLC cell can tailor the monodomain BP and reduce the operating voltage and hysteresis significantly. Low operating voltage owing to higher Kerr constant and a low hysteresis might be due to the exertion of an additional restoring force imparted to the molecules in the cubic geometry by the anchored surfaces. A uniform monodomain also doubles the transmission efficiency and it has better ability to withstand electrostriction.

Acknowledgments This study was supported by the LCD Division of Samsung Electronics and WCU programme R31-20029 through MEST.

1) P. P. Crooker: in *Chirality in Liquid Crystals*, ed. H. S. Kitzerow, C. Bahr, and S. Chandrasekhar (Springer, New York, 2001) Sect. 7, p. 186.
2) S. Meiboom *et al.*: Phys. Rev. A **28** (1983) 3553.
3) P. P. Crooker: Liq. Cryst. **5** (1989) 751.
4) P. E. Cladis: in *Theory and Applications of Liquid Crystals*, ed. J. L. Ericksen and D. Kinderlehrer (Springer, New York, 1987) p. 73.
5) H. Stegemeyer *et al.*: Liq. Cryst. **1** (1986) 3.
6) R. Barbet-Massin *et al.*: Phys. Rev. A **30** (1984) 1161.
7) M. J. Costello *et al.*: Phys. Rev. A **29** (1984) 2957.
8) H. Lee *et al.*: SID Symp. Dig. Tech. Pap. **42** (2011) 121.
9) K. M. Chen *et al.*: J. Disp. Technol. **6** (2010) 49.
10) Z. Ge *et al.*: J. Disp. Technol. **5** (2009) 250.
11) H. Kikuchi *et al.*: SID Symp. Dig. Tech. Pap. **40** (2009) 578.
12) K. M. Chen *et al.*: J. Disp. Technol. **6** (2010) 318.
13) H. Kikuchi *et al.*: Nat. Mater. **1** (2002) 64.
14) M. Kim *et al.*: J. Phys. D **42** (2009) 235502.
15) S. Yoon *et al.*: Liq. Cryst. **37** (2010) 201.
16) J. Yan and S.-T. Wu: SID Symp. Dig. Tech. Pap. **42** (2011) 210.
17) A. Mukherjee *et al.*: Liq. Cryst. **39** (2012) 231.
18) W. Cao *et al.*: Nat. Mater. **1** (2002) 111.
19) Y. Hisakado *et al.*: Adv. Mater. **17** (2005) 96.
20) A. Tiribocchi *et al.*: Soft Mater. **7** (2011) 3295.
21) P. Weinberger: Philos. Mag. Lett. **88** (2008) 897.
22) S.-W. Choi *et al.*: Opt. Mater. **32** (2009) 190.